Title

Ovarian effects of prenatal exposure to benzo[a]pyrene: Roles of embryonic and maternal glutathione status

Authors

Luderer, Ulrike
Myers, Meagan B
Banda, Malathi
et al.

Publication Date

2017-04-01

DOI

10.1016/j.reprotox.2017.03.001

Ovarian Effects of Prenatal Exposure to Benzo[a]pyrene: Roles of Embryonic and Maternal Glutathione Status

[1,2,3,4]Ulrike Luderer, [5]Meagan B. Myers, [5*]Malathi Banda, [5]Karen L. McKim, [1]Laura Ortiz, [5]Barbara L. Parsons

Keywords: polycyclic aromatic hydrocarbon, Kras, puberty, ovarian follicles, mutation, glutathione

[1]Division of Occupational and Environmental Medicine, Department of Medicine, University of California Irvine, Irvine, CA 92617; [2]Department of Developmental and Cell Biology, UC Irvine, Irvine, CA 92617; [3]Program in Public Health, UC Irvine, Irvine, CA 92617; [5]U.S. Food and Drug Administration, Division of Genetic and Reproductive Toxicology, National Center for Toxicological Research, Jefferson, AR

Corresponding author:
Dr. Ulrike Luderer
Center for Occupational and Environmental Health
University of California Irvine
100 Theory Drive, Suite 100
Irvine, CA 92617-1830

Email: uluderer@uci.edu
Tel: +1 (949) 824-8641
Fax: +1 (949) 824-2345

Current Affiliation:
Dr. Malathi Banda
Genetic Toxicology
Covance, Inc
Greenfield, IN 46140-5006
Malathi.Banda@covance.com

Abstract

Females deficient in the glutamate cysteine ligase modifier subunit (*Gclm*) of the rate-limiting enzyme in glutathione synthesis are more sensitive to ovarian follicle depletion and tumorigenesis by prenatal benzo[a]pyrene (BaP) exposure than *Gclm+/+* mice. We investigated effects of prenatal exposure to BaP on reproductive development and ovarian mutations in *Kras*, a commonly mutated gene in epithelial ovarian tumors. Pregnant mice were dosed from gestational day 6.5 through 15.5 with 2 mg/kg/day BaP or vehicle. Puberty onset occurred 5 days earlier in F1 daughters of all *Gclm* genotypes exposed to BaP compared to controls. *Gclm+/-* F1 daughters of *Gclm+/-* mothers and wildtype F1 daughters of wildtype mothers had similar depletion of ovarian follicles following prenatal exposure to BaP, suggesting that maternal *Gclm* genotype does not modify ovarian effects of prenatal BaP. We observed no BaP treatment or *Gclm* genotype related differences in ovarian *Kras* codon 12 mutations in F1 offspring.

Introduction

Polycyclic aromatic hydrocarbons (PAHs), such as benzo[a]pyrene (BaP), are formed during the incomplete combustion of organic materials like fossil fuels, wood, tobacco, and foods [1]. PAH exposure occurs primarily via inhalation of polluted air and tobacco smoke and consumption of grilled and smoked foods [2, 3]. Biomonitoring data show that PAH exposure is ubiquitous [4-6].

Many PAHs, including BaP, are mutagenic and carcinogenic. BaP is classified as a known human carcinogen, causing cancer by inhalation, ingestion, and dermal routes of exposure [7]. Mutagenicity of PAHs is generally thought to require metabolic activation. Mutagenic products of Phase I BaP metabolism include BaP diol epoxide, radical cations, and reactive oxygen species [8-12]. Glutathione-*S*-transferase mediated conjugation with glutathione (GSH) is an important detoxification pathway for PAH diol epoxides and their precursor metabolites [13-16]. GSH together with glutathione peroxidases is also critically important for detoxification of reactive oxygen species generated during PAH metabolism [17, 18].

Experimental studies have shown that postnatal exposure to BaP and several other PAHs destroys ovarian follicles, causing premature ovarian failure [19-22]. Ovarian failure is thought to play a role the pathophysiology of ovarian cancer, and postnatal BaP exposure also causes ovarian tumors in experimental animals [23-25]. The developing ovary is more sensitive than the postnatal ovary to destruction of germ cells by BaP [26, 27]. We previously showed that developing mice deficient in GSH due to deletion of the modifier subunit of glutamate cysteine ligase (*Gclm-/-* mice), the rate limiting enzyme in GSH synthesis, have increased sensitivity to the transplacental ovarian toxicity of BaP, showing greater depletion of ovarian germ cells, lower fertility, and higher incidence of epithelial ovarian tumors than *Gclm+/+* littermates [27].

Ninety percent of malignant ovarian cancers in women are epithelial ovarian cancers [28]. Mutations in oncogenes and tumor suppressor genes are considered obligate events in the development of epithelial ovarian cancers in humans. In particular, mutations in the *KRAS* oncogene have been associated with mucinous epithelial ovarian tumors [29], which are the type of epithelial ovarian tumor most strongly associated with smoking [30, 31]. Although *TRP53* is the most commonly found mutated gene in epithelial ovarian cancers overall, *KRAS* mutations are the second most frequent mutations observed in these cancers [32]. *KRAS* is an attractive target for investigating exposure-related mutational impacts because most of the *KRAS* mutations (~90%) are localized within codon 12. In fact, two specific *KRAS* base substitution mutations account for more than 70% of all reported ovarian carcinoma *KRAS* mutations, *KRAS* codon 12 GAT (G12D, 39.7%) and codon 12 GTT (G12V, 32.2%). KRAS is a GTPase that regulates cell proliferation and survival, and mutation in codon 12 results in enhanced GTP binding, which increases constitutive activity [33]. Because *KRAS* mutation has been identified in benign and malignant mucinous tumors, it has been concluded that *KRAS* mutation is an early event in mucinous ovarian tumorigenesis [34].

Allele-specific Competitive Blocker Polymerase Chain Reaction (ACB-PCR) is a sensitive allele-specific PCR method that has the ability to quantify specific basepair

substitution mutations in a DNA sample at frequencies at or above three mutant alleles per 300,000 wild-type (WT) alleles (sensitivity of 10^{-5}) [35]. ACB-PCR has been used to demonstrate that human tumors frequently possess subpopulations of *KRAS* mutant cells, which are not detected by DNA sequencing [36-39]. This indicates that *KRAS* mutation likely contributes to carcinogenesis to a greater extent than can be recognized by DNA sequence analyses.

ACB-PCR has been used to study the early effects of potentially carcinogenic chemical exposures in rodents [40]. For example, ACB-PCR was used to detect a significant induction of *Kras* mutation in the lungs of A/J mice that received a single i.p. injection of BaP [41]. In fact, a significant induction of mutation was observed at a ten-fold lower dose than that which produced a significant lung tumor bioassay response. In human lung, induction of *KRAS* codon 12 G to T mutation has been associated with cigarette smoking [42].

Given that 1) ACB-PCR detected significant induction of *Kras* mutation in BaP exposed mouse lung [41], 2) deletion of the *Gclm* gene oxidizes the GSH redox state of the mouse ovary [43], 3) *Gclm-/-* F1 female offspring of *Gclm+/-* mothers treated with BaP during pregnancy have increased sensitivity to BaP-induced epithelial ovarian tumors compared to *Gclm+/+* littermates [27], and 4) *Kras* mutant cell selection may be impacted by oxidative stress [38], we sought to determine whether and/or how B*a*P treatment, in the context of *Gclm* genotype, would impact *Kras* codon 12 GAT and GTT mutation levels in mouse ovary and whether maternal *Gclm+/-* genotype plays any role in the transplacental ovarian toxicity of BaP.

Methods

Materials

All chemicals and reagents were purchased from Fisher Scientific or Sigma Aldrich unless otherwise noted.

Animals

Generation of mice in which exon 1 of the *Gclm* gene was deleted was previously described [44, 45]. These mice are maintained on a C57BL/6J genetic background at the University of California Irvine [46]. Mice were housed in an American Association for Laboratory Animal Medicine accredited vivarium, on a 14 h light, 10 h dark cycle. Temperature was maintained at 69-75°F. Animals had free access to autoclaved, deionized water and irradiated, soy-free rodent chow (Harlan Teklad 2919).

Experimental Design

For assessment of F1 ovarian oncomutations and the timing of puberty after prenatal exposure to BaP, adult 10-16 week old *Gclm+/-* females were placed with adult *Gclm+/-* males on the afternoon of proestrus of the estrous cycle determined by vaginal cytology (see below). The next morning, the females were checked for vaginal plugs and separated from the males. If no plug was found, vaginal cytology was continued and the female was mated again on the next proestrus. The day a plug was found was

designated gestational day (GD) 0.5. The females were orally dosed once daily on GD 6.5 to 15.5 with 2 mg/kg BaP (Sigma-Aldrich Supelco, St Louis, MO; 99% purity) dissolved in sesame oil or sesame oil alone (n=10 each). The dose was chosen because it caused submaximal effects on the ovaries of *Gclm+/+* mice in our earlier study [27], enabling demonstration of greater sensitivity to the prenatal ovarian toxicity in *Gclm-/-* mice. The dosing volume was held constant at 1mL/kg.

Pregnant females were allowed to give birth and nurse their offspring until weaning on post-natal day (PND) 21. After weaning, female F1 offspring were group-housed up to 4 per cage. Beginning on PND 21, all F1 females were checked daily for vaginal opening; starting on the day of vaginal opening, they underwent vaginal lavage with 0.9% sodium chloride solution daily for assessment of estrous cycling until the first estrus (cytology with abundant cornified cells; [47]) to determine the onset of puberty. All F1 females were weighed on the days of weaning, vaginal opening, and first estrus. At most 1 *Gclm-/-* female, 1 *Gclm+/-* female and 1 *Gclm*+/+ female per litter were euthanized on the first vaginal estrus (PND 34-46) by CO_2 narcosis, followed by transection of the diaphragm. We euthanized mice on first estrus for several reasons. First, we thought it was more important for all of the mice to be at the same developmental stage at the time of euthanasia than to be exactly the same chronological age. Second, at this age the ovaries of BaP-exposed mice are not yet devoid of follicles and show no signs of tumor development. Ovaries were harvested and snap frozen on dry ice for quantification of *Kras* codon 12 mutations (N=5-7 per each of the six experimental groups). A second *Gclm+/-* female per litter was euthanized on first estrus and one ovary plus oviduct was processed for histomorphometry.

For assessment of the effect of prenatal BaP exposure on ovarian follicle counts in the F1 offspring of wild type mothers, the identical mating and dosing procedures were used with wild type C57BL/6J mice (purchased from Jackson Laboratories, Bar Harbor, ME) and acclimated for at least one week prior to mating. F1 female offspring were euthanized as above at 6 weeks of age (PND 42 to 49). One ovary and oviduct from each mouse was processed for histomorphometry.

All procedures involving animals followed established guidelines [48] and were approved by the Institutional Animal Care and Use Committee of the University of California Irvine.

Ovarian histomorphometry

Ovary plus oviduct was fixed in Bouin's fixative (Electron Microscopy Sciences, Hatfield, PAH) at 4°C for 24h, rinsed in 50% ethanol, washed in 50% ethanol for 30-60 min three times, and stored in 70% ethanol. Ovaries were embedded in paraffin, serially sectioned at 5 μm thickness, and stained with hematoxylin and eosin. Every serial section was evaluated in a blinded manner, as previously described [43]. Briefly, follicles with a visible nucleus (primordial and small primary) or nucleolus (larger follicles) were classified as primordial (single layer of fusiform granulosa cells), primary (single layer with two or more cuboidal granulosa cells), secondary (greater than one layer of granulosa cells with no antrum), or antral [49, 50]. Primordial, primary, and secondary follicles were counted in every 5th section; the sums of the counts were

multiplied times five to estimate the total number per ovary. Antral follicles and corpora lutea were counted in every section, taking care to count each of the latter structures only once.

DNA isolation

Ovaries were separated from oviducts, snap frozen on dry ice, and stored at -80°C until shipment on dry ice to the National Center for Toxicological Research (Jefferson, AR). There, ovaries were homogenized in 0.2 ml of extraction buffer, consisting of 0.5 mg/ml proteinase K, 20 mM NaCl, 1 mM $CaCl_2$, and 10 mM Tris pH 8.0. Samples were incubated ~16 hrs at 37°C, then extracted with an equal volume of phenol/chloroform/isoamyl alcohol (25:24:1) and ethanol-precipitated. Samples were resuspended in 100 µl of RNase buffer: 10 mg/ml RNase A (Sigma, St. Louis, MO), 600 units/ml Ribonuclease T1 (Sigma), 100 mM sodium acetate, and 50 mM Tris-HCl (pH 8), incubated ~16 hours at 37 °C, then re-extracted with phenol/chloroform/isoamyl alcohol as described above. Each DNA sample was ethanol precipitated, then resuspended in 50 µl of TE buffer (5 mM Tris, 0.5 mM EDTA, pH 7.5). DNA samples were digested with HindIII according to the manufacturer's instructions (New England Biolabs, Beverly, MA). Finally, the DNA was phenol/chloroform/isoamyl alcohol extracted as described above, ethanol-precipitated and resuspended in 40 µl of TE buffer. DNA concentrations were measured spectrophotometrically.

Preparation of standards and unknowns by first-round PCR amplification

PfuUltra hotstart high-fidelity DNA polymerase (Stratagene, La Jolla, CA) was used to generate first-round PCR products encompassing *Kras* codon 12 from the HindIII-digested mouse ovary genomic DNA samples and from linearized plasmid DNAs carrying the mutant or WT *Kras* sequence to use as MF standards.

Specifically, a 170 bp gene segment encompassing part of the 5' untranslated region, exon 1, and part of intron 1 (NC_000072 Region: 29,950 to 30,119) was amplified. Each 200-µl PCR amplification reaction contained: 1 µg genomic DNA, 200 nM primer TR67 (TR67, 5'-TGGCTGCCGTCCTTTACAA-3'), 200 nM primer TR68 (TR68, 5'-GGCCTGCTGAAAATGACTGAGTATAAACTTGT-3'), 200 nM dNTPs, 1X *PfuUltra* reaction buffer, and 10 units *PfuUltra* hotstart high-fidelity DNA Polymerase (Stratagene). Cycling conditions were 94°C for 2 min, followed by 28 cycles of 94°C for 1 min, 58°C for 2 min, 72°C for 1 min, followed by a 7 min extension at 72°C. Primers were purchased from Integrated DNA Technologies, Coralville, IA.

Purification of and quantification of PCR products

The PCR products (standards and unknowns) were purified by ion-pair reverse phase chromatography using a WAVE Nucleic Acid Fragment Analysis System (Transgenomic, Omaha, NE). PCR products were complexed with 0.1 M triethylammonium acetate (Buffer A: 0.1M TEAA) and bound to a DNASep column (containing C18 alkylated PS/DVB polymer). PCR products, input template, unincorporated nucleotides, and primers were eluted using a gradient of increasing

acetonitrile concentration (Buffer B: 0.1 M TEAA, 25% acetonitrile), thereby separating nucleic acids by size/column retention time. A threshold collection method was used to collect the 170 bp PCR products based on their absorbance at 260 (measured with a UV detector at the appropriate retention time) into individual tubes in a chilled fraction collector. PCR products were evaporated to dryness using a Savant Speed-Vac Concentrator (Model ISS110, Thermo Fisher Scientific, Rockville, MD), then resuspended in TE buffer and multiple 2-µl aliquots were prepared and stored at -80°C. Aliquots were quantified using an Epoch Micro-Volume Spectrophotometer System with a Take3 Microplate Reader (Biotek Instruments, Winooski, VT), until three measurements that varied by <10% from the group mean were obtained.

ACB-PCR quantification of Kras codon 12 GAT and GTT MF in mouse ovary DNA

Purified mutant and WT first-round PCR products were combined to generate mutant fraction (MF) standards with mutant: WT ratios of 10^{-1}, 10^{-2}, 10^{-3}, 10^{-4}, 10^{-5}, and 0 (no-mutant control). MF is the ratio of mutant to wild-type alleles in a given DNA sample, in this instance the ratio of alleles mutated at *KRAS* codon 12 (GAT or GTT) to *KRAS* codon 12 wild type alleles (GGT). Duplicate MF standards and a no-DNA control were analyzed in parallel with first-round PCR products synthesized from mouse ovary DNA, each assay being conducted using 5 X 10^8 total copies of first-round product. ACB-PCR was performed using 50 µl reactions in 96-well plates and a DNA Engine Tetrad 2 (Bio-Rad Life Science Research, Hercules, CA). Each *Kras* codon 12 GAT ACB-PCR reaction contained: 1X Standard Taq (Mg-free) reaction buffer (New England Biolabs), 0.1 mg/ml gelatin, 1 mg/ml Triton X-100, 40 µM dNTPs, 1.6 mM $MgCl_2$, 160 nM mutant-specific primer (TR76, 5'-fluorescein-CTTGTGGTGGTTGGAGCTAA-3'), 525 nM blocker primer (TR112, 5'-CTTGTGGTGGTTGGAGCTAdG-3'), and 150 nM upstream primer (TR111, 5'-GTAGGGTCATACTCATCCAC-3'). Each reaction was initiated with the addition of 0.3 µg of Extreme Thermostable Single-stranded DNA Binding Protein (New England Biolabs, Beverly, MA), 33 mUnits of PerfectMatch PCR Enhancer, and 65 mUnits of Hemo KlenTaq DNA polymerase (New England Biolabs). Cycling conditions were 2 min at 94°C, followed by 36 cycles of 94°C for 30 sec, 45°C for 90 sec, and 68°C for 1 min. The *Kras* codon 12 GAT ACB-PCR product is 89 bp in length. Each *Kras* codon 12 GTT ACB-PCR reaction contained: 1X Standard Taq (Mg-free) reaction buffer, 0.1 mg/ml gelatin, 1 mg/ml Triton X-100, 40 µM dNTPs, 1.5 mM $MgCl_2$, 400 nM mutant-specific primer (TR87, 5'-fluorescein-CTTGTGGTGGTTGGAGCTAT-3'), 440 nM blocker primer (TR113, 5'-CTTGTGGTGGTTGGAGCTTG-3'-phosporylation, purchased from Biosynthesis, Lewisville, TX), and 400 nM upstream primer (TR110, 5'-TCGTAGGGTCATACTCATC-3'). Each reaction was initiated with the addition of 160 mUnits of PerfectMatch PCR Enhancer (Stratagene), and 70 mUnits of Hemo KlenTaq DNA polymerase. Cycling conditions were 2 min at 94°C, followed by 36 cycles of 94°C for 30 sec, 41°C for 90 sec, and 68°C for 1 min. The *Kras* codon 12 GTT ACB-PCR product is 91 bp in length.

Gel electrophoresis and quantification of ACB-PCR products

Following ACB-PCR, 10 µl of bromophenol blue/xylene cyanol-containing 6X ficoll loading dye was added to each well of the 96-well plate, mixed, and 10 µl of each ACB-PCR reaction product was loaded onto an 8% non-denaturing polyacrylamide gel. Fluorescein-labeled, ACB-PCR products of the correct-size were quantified using a PharosFX scanner with an external blue laser (Bio-Rad). Pixel intensities of the bands were quantified using Quantity One® software and a locally-averaged background correction (Bio-Rad).

Data Analyses

The effects of genotype and BaP dose on the continuous outcome variables age and weight at vaginal opening and first vaginal estrus were analyzed using Generalized Estimating Equations, a form of Generalized Linear Models, with BaP dose, *Gclm* genotype, and BaP x genotype interaction modeled as fixed effects. In order to adjust for litter effects, litter numbers were entered into the model as a subject effect using an unstructured working correlation matrix structure.

Differences in ovarian follicle counts between prenatally vehicle-exposed compared to BaP-exposed groups were analyzed by *t*-test for equal or unequal variances as appropriate.

For *Kras* codon 12 GAT MF determination, the pixel intensities of the MF standards (10^{-2} to 10^{-5}) were plotted against their MFs on log-log plots. A trend line (power function) was fitted to the data and the function was used to calculate the MF in each unknown sample based on its pixel intensity. The arithmetic average of the three independent MF measurements was calculated. The average MF in each mouse ovary DNA sample was log-transformed and the average log-transformed MF for BaP-treated and control mice were calculated (geometric mean MF for each treatment group). For *Kras* codon 12 GTT MF determination, the procedure was the same, except pixel intensities of the MF standards were plotted against their MFs using log-linear plots and the trend line was a logarithmic function.

Two-way analysis of variance was performed to test for differences in *Kras* MF related to BaP-treatment or *Gclm* genotype. An unpaired T-test was used to compare the levels of *Kras* codon 12 GAT and GTT mutation within mouse ovary DNA samples. Pearson product-moment correlation coefficient was determined to test for a correlation between the Log_{10} MF *Kras* codon 12 GAT and GTT MFs within individual mouse ovary DNA samples.

Results

Effects of prenatal BaP exposure and Gclm genotype on timing of puberty

In view of the pronounced effects of prenatal BaP exposure on ovarian follicle number and fertility in adulthood that we observed previously, we were interested in determining whether prenatal BaP exposure also alters the timing of puberty. First estrus is considered to be a more reliable indicator of the onset of puberty in mice than vaginal opening [51] because age at vaginal opening does not coincide with first estrus in mice as it does in rats [52]. The mean ages at vaginal opening are shown in Figure 1A. There was no statistically significant effect of prenatal BaP dose on age at vaginal

opening, but age at vaginal opening varied significantly with *Gclm* genotype and with the BaP dose by genotype interaction (P<0.001). This was because age at vaginal opening was later in the *Gclm-/-* females, but the delay in vaginal opening was blunted by prenatal BaP exposure. Age at first estrus occurred about 5 days earlier on average in all *Gclm* genotypes exposed to BaP *in utero*, compared to oil-exposed controls of the same genotype (P<0.001, effect of BaP; Figure 1B), and there was no significant effect of genotype or dose by genotype interaction. Weight at vaginal opening varied significantly with BaP dose, genotype, and with their interaction (P≤0.005), with higher weight at vaginal opening in the *Gclm+/+* and *Gclm+/-* mice, but not in the *Gclm-/-* mice. Weight at first estrus varied significantly with BaP dose (P=0.014), genotype (P<0.001), and with their interaction (P<0.001). Weight at first estrus was higher on average by about 1 g in the BaP exposed *Gclm+/+* and *Gclm+/-* mice, but was about 0.5 g lower in the BaP-exposed *Gclm-/-* mice compared to their respective oil controls.

Maternal Gclm heterozygosity does not enhance the effects of in utero BaP exposure on follicle numbers in daughters

For comparison of the effects of prenatal BaP on ovarian follicle counts in the *Gclm+/-* daughters of *Gclm+/-* mothers and fathers with follicle counts in wild type daughters of wild type parents, one F1 *Gclm+/-* female was randomly chosen from each of 4 control litters and one was chosen from each of 5 BaP-exposed litters. Follicle counts are shown in Figure 2. Numbers of primordial follicles were 71% lower in BaP-exposed *Gclm+/-* F1 offspring of *Gclm+/-* mothers (Figure 2A; P=0.036) and 81% lower in wild type F1 offspring of wild type mothers (Figure 2B; P=0.005) compared to respective controls. The effects of prenatal BaP exposure on numbers of healthy primary, secondary, and antral follicles were also similar between the two experiments (Figure 2C-H). Numbers of follicles of all stages combined were 66% decreased in BaP-exposed wild type offspring of wild type dams and 65% decreased in BaP-exposed *Gclm+/-* offspring of *Gclm+/-* dams compared to respective controls. Similar differences were seen in the numbers of atretic follicles at each follicle stage, with fewer atretic follicles in BaP-exposed compared to controls in the two experiments (data not shown). Thus, the effect of prenatal BaP on F1 ovarian follicle numbers does not appear to be affected by maternal *Gclm+/-* versus wild type genotype.

Neither prenatal exposure to BaP nor Gclm genotype affects ovarian Kras codon 12 mutation fractions

In order to avoid developmental stage-related differences in follicle types and numbers and presence or absence of corpora lutea in the ovaries of mice harvested for histomorphometry or for mutation analysis, we euthanized the mice on the first vaginal estrus. ACB-PCR was used to measure the *Kras* codon 12 GAT and GTT MFs in the ovarian DNA of mice of three different genotypes, *Gclm*+/+, *Gclm*+/-, and *Gclm-/-* that had been transplacentally exposed to BaP or vehicle (Figure 3A). The individual treatment groups were comprised of five to seven individual mouse ovary DNA samples, each derived from a different, transplacentally exposed litter (Figure 3B). Figure 4 shows the MF distributions for each *Kras* mutation in the different treatment groups. The *Kras* codon 12 GAT and GTT geometric mean MFs and median MFs for each treatment group are provided in Table 1. Two-way analysis of variance was employed to test for differences in *Kras* MF related to BaP-treatment or *Gclm* genotype.

No significance differences in *Kras* codon 12 GAT or GTT MF related to B[a]P-treatment, *Gclm* genotype, or their interaction were observed. Interestingly, the data in Table 1 indicate that mouse ovary samples have greater levels of *Kras* codon 12 GTT than GAT mutation, which is unusual because most human and rodent tissues generally have been found to carry greater levels of the GAT than GTT mutation [38, 53-55]. In order to investigate this observation further, and because no significant differences related to treatment or genotype were detected, the *Kras* codon 12 GTT MF measurements were combined and compared to the GAT MF measurements using an unpaired T-test. This analysis demonstrated that there are significantly greater levels of *Kras* codon 12 GTT mutations than GAT mutations in mouse ovary DNA ($P = 0.0088$, two-tailed test). Furthermore, a significant correlation was observed between the *Kras* codon 12 GAT and GTT Log_{10} MF measurements within individual mouse ovary DNA samples (Pearson $r=0.8504$, $P<0.0001$, two-tailed test; Figure 5).

Discussion

Prenatal exposure to BaP from GD 6.5 to 15.5, during the period of gonadal differentiation through meiosis onset in the ovary, depletes germ cells, leading to premature ovarian failure, decreased fertility, and ovarian tumors in later life, and *Gclm-/-* females are more sensitive to all these effects [26, 27]. The results of the present study show that the same prenatal BaP regimen results in 5 day earlier onset of puberty (first vaginal estrus) in F1 female offspring regardless of *Gclm* genotype. Moreover, this regimen causes similar depletion of germ cells in wild type F1 female offspring of wild type dams as in *Gclm+/-* F1 female offspring of *Gclm+/-* dams, suggesting that maternal *Gclm* heterozygosity does not modify the ovarian effects of prenatal exposure to BaP. We also for the first time measured *Kras* codon 12 mutations in the ovary. We found that neither codon 12 GAT nor GTT mutation was increased in the ovaries of mice of all three *Gclm* genotypes after prenatal exposure to BaP, but, in contrast to other tissues, we observed that ovarian levels of GTT mutations were higher than GAT mutations.

To our knowledge, this is the first study to examine the effects of prenatal exposure to any PAH on the timing of puberty in female mice. We previously reported that prenatal exposure to BaP increases adiposity and postnatal weight gain in *Gclm+/+* F1 female offspring, but not *Gclm-/-* F1 offspring [56]. Although puberty is well-known to be linked to body weight [51], the effect of BaP on age at puberty in the present study cannot be explained by effects of BaP on body weight alone. Age at first estrus occurred about 5 days earlier in mice of all *Gclm* genotypes after prenatal BaP exposure, while weight at first estrus was increased in BaP-exposed *Gclm+/+ and Gclm+/-* F1 females and decreased in BaP-exposed *Gclm-/-* F1 females. This suggests that the earlier onset of puberty was not mediated by accelerated postnatal weight gain. The ages at vaginal opening and first estrus in control mice in the present study are consistent with prior published data in the C57BL/6J strain [57, 58]. *In utero* exposure to estradiol and xenoestrogens such as the insecticide methoxychlor also results in earlier onset of puberty [59-61]. Several studies have demonstrated estrogenic activity of BaP or its metabolites, mediated by estrogen receptor activation [62, 63]. Therefore, we hypothesize that the mechanism by which *in utero* exposure to BaP advances puberty involves estrogen receptor signaling.

We examined the potential modifying effect of maternal *Gclm* heterozygosity on ovarian effects of transplacental BaP because *Gclm* heterozygosity has been reported to modify the effects of some toxicant exposures. For example, *Gclm+/-* female mice were more sensitive to pulmonary inflammation from inhalation of diesel exhaust than *Gclm+/+* females [64]. We observed no evidence of modification of the depletion of ovarian follicles by prenatal BaP exposure by maternal *Gclm* genotype in the present study. The ED_{50} for transplacental primordial follicle depletion by BaP in wild type offspring of wild type C57BL/6J dams and in *Gclm+/-* offspring of *Gclm+/-* dams in the present study is clearly less than 2 mg/kg/day, administered from GD6.5 to GD15.5 to the dam (cumulative dose of 20 mg/kg). In contrast, the ED_{50} for primordial follicle depletion in peripubertal female mice dosed daily from postnatal day 28 to 42 was 3 mg/kg/day (cumulative dose of 45 mg/kg) [20]. Moreover, we previously reported that ovarian follicle numbers did not differ between dams dosed with 0 or 10 mg/kg/day from GD6.5-15.5 (cumulative dose of 100 mg/kg) [27]. Taken together these findings show that the developing ovary is more sensitive to germ cell depletion than the peripubertal or adult ovary.

Comparisons of *KRAS* codon 12 GAT (G12D) and GTT (G12V) MF in a variety of human and rodent tissues has demonstrated that the *KRAS* codon 12 GAT mutation is generally the more abundant spontaneous mutation, often present in normal human or control rodent tissues at frequencies up to ten-fold greater than the *KRAS* codon 12 GTT (G12V) mutation [37, 38, 54, 55]. In contrast, we observed significantly higher levels of GTT mutations than GAT mutations in the mouse ovary in the present study. Evaluation of more than one mutation by ACB-PCR has been used as a paradigm to detect chemical-specific effects on mutation frequency. In the rat colon cancer model, for example, azoxymethane induced *Kras* codon 12 GAT mutations, but not codon 12 GTT mutations, which was consistent with the mutational specificity expected for azoxymethane [54]. Conversely, Big Blue rats treated with *N*-hydroxy-2-acetylaminofluorene (*N*-OH-AAF) had significantly increased levels of both mutations in liver DNA, even though induction of G to T mutation was the primary mutational specificity observed in the *LacI* neutral reporter gene of the liver DNA from the same rats. This suggests that in this case N-OH-AAF may have caused amplification of pre-existing *Kras* mutation [55]. We previously reported that treatment of adult male mice with BaP dose-dependently increased *Kras* codon 12 GAT and TGT mutations in lungs [41]. We did not measure the TGT mutation in the present study. However, we do not consider it likely that TGT mutations were increased in the ovaries in the absence of increases in GAT mutations since the increase in GAT and TGT lung mutations after BaP treatment was similar in our prior study.

In the lung tissue of mice exposed to ethylene oxide by inhalation, ACB-PCR detected a biphasic response in levels of *Kras* mutation, meaning an initial induction of mutation was followed by a decrease in *Kras* mutation with longer exposures and higher cumulative doses of ethylene oxide [53]. This led to the suggestion that *Kras* mutant cells may be selected against under some circumstances, possibly those involving oxidative stress. The observations that human *KRAS* codon 12 GTT (G12V) MF decreases during human colonic adenoma to adenocarcinoma progression [37] and that *KRAS* codon 12 G12V MF is inversely proportional to the maximum tumor dimension of colon tumors and papillary thyroid tumors [38] are consistent with the idea that oxidative

stress in hypoxic tumors selects against *KRAS* G12V mutation. However, in the present study, we did not observe decreased GTT MF in the ovaries of *Gclm-/-* mice, despite our prior observations of chronic ovarian oxidative stress in the ovaries of these mice measured by decreased ratio of reduced to oxidized GSH, more oxidized Nernst potential of the GSH/GSSG redox couple, and increased immunostaining for markers of oxidative protein and lipid damage [43]. Our results therefore suggest that factors other than oxidative stress may be responsible for the inverse associations of *KRAS* codon 12 GTT MF with tumor progression in some animal models and human tumors.

In summary, prenatal exposure to BaP during ovarian differentiation decreases ovarian follicle numbers and causes earlier onset of puberty in F1 female offspring. Maternal *Gclm* genotype does not modify the effects of prenatal BaP exposure on ovarian follicle numbers. We found no effects of prenatal BaP exposure or *Gclm* genotype of the F1 offspring on levels of ovarian *Kras* codon 12 mutations. This suggests that the induction of epithelial ovarian tumors by prenatal BaP and the greater sensitivity of *Gclm-/-* females to this effect [27] are not mediated by these *Kras* mutations. Future studies should examine the ovaries of prenatally exposed offspring for other mutations associated with PAH exposure.

Acknowledgments

The authors thank Jeff Kim for embedding and serially sectioning the ovaries for histomorphometry. We thank undergraduate students Jennifer Welch, Christine Pham, Angelica del Rosario, and Muzi Lu for assisting with breeding, assessment of puberty, and vaginal cytology of the mice for this study. The information in these materials is not a formal dissemination of information by FDA and does not represent agency position or policy.

Funding

This work was supported by the National Institutes of Health (NIH) grant R01ES020454 to UL; the University of California Cancer Research Coordinating Committee, grant CRR-12-201314 to UL; and the Center for Occupational and Environmental Health, UC Irvine.

References

[1] ATSDR. Toxicological Profile for Polycyclic Aromatic Hydrocarbons. Atlanta, GA: US Department of Health and Human Services, Public Health Service, Agency for Toxic Substances and Disease Registry; 1995.

[2] Menzie CA, Potocki BB, Santodonato J. Ambient Concentrations and Exposure to Carcinogenic PAHs in the Environment. Environ Sci Technol. 1992;26:1278-84.

[3] Shopland DR, Burns DM, Benowitz NL, Amacher RH. Risks Associated with Smoking Cigarettes with Low Machine-Measured Yields of Tar and Nicotine. Smoking and Tobacco Control Monographs: U.S. Department of Health and Human Services, Public Health Service, National Institutes of Health, National Cancer Institute; 2001. p. 1-236.

[4] NHANES. Fourth National Report on Human Exposure to Environmental Chemicals. Department of Health and Human Services, Centers for Disease Control and Prevention; 2009.

[5] Aquilina NJ, Delgado-Saborit JM, Meddings C, Baker S, Harrison RM, Jacob PI, et al. Environmental and Biological Monitoring of Exposures to PAHs and ETS in the General Population. Environ Int. 2010;36:763-71.

[6] Health Canada. Third Report on Human Biomonitoring of Environmental Chemicals in Canada. Ottawa, CA: Health Canada; 2015.

[7] IARC. Benzo[*a]pyrene*. Chemical Agents and Related Occupations. Lyon, France: International Agency for Research on Cancer, World Health Organization; 2009.

[8] Denissenko MF, Pao A, Tang M-S, Pfeifer GP. Preferential Formation of Benzo[a]pyrene Adducts at Lung Cancer Mutational Hotspots in P53. Science. 1996;274:430-2.

[9] Shimada T, Fujii-Kuriyama Y. Metabolic Activation of Polycyclic Aromatic Hydrocarbons to Carcinogens by Cytochromes P450 1A1 and 1B1. Cancer Sci. 2004;95:1-6.

[10] Xue W, Warshawsky D. Metabolic Activation of Polycyclic Aromatic Hydrocarbon and Heterocyclic Aromatic Hydrocarbons and DNA Damage: A Review. Toxicol Appl Pharmacol. 2005;206:73-93.

[11] Burczynski ME, Penning TM. Genotoxic Polycyclic Aromatic Hydrocarbon *ortho*-Quinones Generated by Aldo-Keto Reductases Induce CYP1A1 via Nuclear Translocation of the Aryl Hydrocarbon Receptor. Cancer Res. 2000;60:908-15.

[12] Penning TM. Aldo-Keto Reductases and Formation of Polycyclic Aromatic Hydrocarbon *o*-Quinones. Methods Enzymol. 2004;378:31-67.

[13] Seidel A, Friedberg T, Löllman B, Schwierzok A, Funk M, Frank H, et al. Detoxification of Optically Active Bay- and Fjord-Region Polycyclic Aromatic Hydrocarbon Dihydrodiol Epoxides by Human Glutathione Transferase P1-1 Expressed in Chinese Hamster V79 Cells. Carcinogenesis. 1998;19:1975-81.

[14] Romert L, Dock L, Jenssen D, Jernström B. Effects of Glutathione Transferase Activity on Benzo[a]pyrene 7,8-dihydrodiol Metabolism and Mutagenesis Studied in a Mammalian Cell Co-cultivation Assay. Cancer Res. 1989;10:1701-7.

[15] Kushman ME, Kabler SL, Fleming MH, S. R, Gupta RC, Doehmer J, et al. Expression of Human Glutathione S-transferase P1 Confers Resistance to Benzo[a]pyrene or Benzo[a]pyrene-7,8-Dihydrodiol Mutagenesis, Macromolecular Alkylation and Formation of Stable N2-Gua-BPDE Adducts in Stably Transfected V79MZ Cells Co-Expressing hCYP1A1. Carcinogenesis. 2007;28:207-14.

[16] Jernström B, Funk M, Frank H, Mannervik B, Seidel A. Glutathione-S-Transferase A1-1-Catalysed Conjugation of Bay and Fjord Region Diol Epoxides of Polycyclic Aromatic Hydrocarbons with Glutathione. Carcinogenesis. 1996;17:1491-8.

[17] Marí M, Morales A, Colell A, García-Ruiz C, Fernández-Checa JC. Mitochondrial Glutathione, a Key Survival Antioxidant. Antioxidants and Redox Signaling. 2009;11:2685-700.

[18] Roberts RA, Laskin DL, Smith CV, Robertson FM, Allen EMG, Doorn JA, et al. Nitrative and Oxidative Stress in Toxicology and Disease. Toxicol Sci. 2009;112:4-16.

[19] Mattison DR, White NB, Nightingale MR. The Effect of Benzo(a)pyrene on Fertility, Primordial Oocyte Number, and Ovarian Response to Pregnant Mare's Serum Gonadotropin. Pediatr Pharmacol. 1980;1:143-51.

[20] Borman SM, Christian PJ, Sipes IG, Hoyer PB. Ovotoxicity in Female Fischer Rats and B6 Mice Induced by Low-Dose Exposure to Three Polycyclic Aromatic Hydrocarbons: Comparison through Calculation of an Ovotoxic Index. Toxicol Appl Pharmacol. 2000;167:191-8.

[21] Mattison DR. Morphology of Oocyte and Follicle Destruction by Polycyclic Aromatic Hydrocarbons in Mice. Toxicol Appl Pharmacol. 1980;53:249-59.

[22] Mattison DR, Thorgeirsson SS. Ovarian Aryl Hydrocarbon Hydroxylase Activity and Primordial Oocyte Toxicity of Polycyclic Aromatic Hydrocarbons in Mice. Cancer Res. 1979;39:3471-5.

[23] Uematsu K, Huggins C. Induction of Leukemia and Ovarian Tumors in Mice by Pulse-Doses of Polycyclic Aromatic Hydrocarbons. Mol Pharmacol. 1968;4:427-34.

[24] Rämet M, Castrén K, Järvinen K, Pekkala K, Turpeenniemi-Hujanen T, Soini Y, et al. p53 Protein Expression is Correlated with Benzo[a]pyrene-DNA Adducts in Carcinoma Cells. Carcinogenesis. 1995;16:2117-24.

[25] Biancifiori C, Bonser GM, Caschera F. Ovarian and Mammary Tumours in Intact C3Hb Virgin Mice Following a Limited Dose of Four Carcinogenic Chemicals. Br J Cancer. 1961;15:270-83.

[26] MacKenzie KM, Angevine DM. Infertility in Mice Exposed in Utero to Benzo(a)pyrene. Biol Reprod. 1981;24:183-91.

551 [27] Lim J, Lawson GW, Nakamura BN, Ortiz L, Hur JA, Kavanagh TJ, et al. Glutathione-
552 Deficient Mice Have Increased Sensitivity to Transplacental Benzo[a]pyrene-Induced Premature
553 Ovarian Failure and Ovarian Tumorigenesis. Cancer Res. 2013;73:908-17.

554 [28] Chen VW, Ruiz B, Killeen JL, Cote TR, Wu XC, Correa CN. Pathology and Classification of
555 Ovarian Tumors. Cancer. 2003;97:2631-42.

556 [29] Matias-Guiu X, Prat J. Molecular Pathology of Ovarian Carcinomas. Virchows Arch.
557 1998;433:103-11.

558 [30] Gates MA, Rosner BA, Hecht JL, Tworoger SS. Risk Factors for Epithelial Ovarian Cancer
559 by Histologic Subtype. Am J Epidemiol. 2010;171:45-53.

560 [31] Rossing MA, Cushing-Haugen KL, Wicklund KG, Weiss NS. Cigarette Smoking and Risk of
561 Epithelial Ovarian Cancer. Cancer Causes Control. 2008;19:413-20.

562 [32] The Cancer Genome Atlas Research Network. Integrated Genomic Analyses of Ovarian
563 Carcinoma. Nature. 2011;474:609-15.

564 [33] Prior IA, Lewis PD, Mattos C. A Comprehensive Survey of Ras Mutations in Cancer.
565 Cancer Res. 2012;72:2457-67.

566 [34] Cuatrecasas M, Villanueva A, Matias-Guiu X, Prat J. K-ras Mutations in Mucinous Ovarian
567 Tumors: A Clinicopathologic and Molecular Study of 95 Cases. Cancer. 1997;79:1581-6.

568 [35] Myers M, McKinzie P, Wang Y, Meng F, Parsons B. ACB-PCR Quantification of Somatic
569 Oncomutation. In: Keohavong P, Grant SG, editors. Molecular Toxicology Protocols. New York,
570 N.Y.: Humana Press; 2014. p. 345-63.

571 [36] Myers MB, McKim KL, Parsons BL. A Subset of Papillary Thyroid Carcinomas Contain
572 KRAS Mutant Subpopulations at Levels above Normal Thyroid. Mol Carcinog. 2014;53:159-67.

573 [37] Parsons BL, Marchant-Miros KE, Delongchamp RR, Verkler TL, Patterson TA, McKinzie
574 PB, et al. ACB-PCR Quantification of K-RAS Codon 12 GAT and GTT Mutant Fraction in Colon
575 Tumor and Non-tumor Tissue. Cancer Invest. 2010;28:364-75.

576 [38] Parsons BL, Myers MB. KRAS Mutant Tumor Subpopulations Can Subvert Durable
577 Responses to Personalized Cancer Treatments. Personalized Medicine. 2013;10:191-9.

578 [39] Myers MB, McKim KL, Meng F, Parsons BL. Low-frequency KRAS mutations are prevalent
579 in lung adenocarcinomas. Personalized Medicine. 2015;12:83-98.

580 [40] Parsons BL, Myers MB, Meng F, Wang Y, McKinzie PB. Oncomutations as Biomarkers of
581 Cancer Risk. Environ Mol Mutagen. 2010;51:836-50.

582 [41] Meng F, Knapp GW, Green T, Ross JA, Parsons BL. K-*Ras* Mutant Fraction in A/J Mouse
583 Lung Increases as a Function of Benzo[a]pyrene Dose. Environ Mol Mutagen. 2010;51:146-55.

584 [42] Gealy R, Zhang L, Siegfried JM, Luketich JD, Keohavong P. Comparison of Mutations in
585 the p53 and K-ras Genes in Lung Carcinomas from Smoking and Nonsmoking Women. Cancer
586 Epidemiol Biomarkers Prev. 1999;8:297-302.

[43] Lim J, Nakamura BN, Mohar I, Kavanagh TJ, Luderer U. Glutamate Cysteine Ligase Modifier Subunit (*Gclm*) Null Mice Have Increased Ovarian Oxidative Stress and Accelerated Age-related Ovarian Failure. Endocrinology. 2015;156:3329-43.

[44] McConnachie LA, Mohar I, Hudson FN, Ware CB, Ladiges WC, Fernandez C, et al. Glutamate Cysteine Ligase Modifier Subunit Deficiency and Gender as Determinants of Acetaminophen-Induced Hepatotoxicity in Mice. Toxicol Sci. 2007;99:628-36.

[45] Giordano G, White CC, McConnachie LA, Fernandez C, Kavanagh TJ, Costa LG. Neurotoxicity of Domoic Acid in Cerebellar Granule Neurons in a Genetic Model of Glutathione Deficiency. Mol Pharmacol. 2006;70:2116-26.

[46] Nakamura BN, Fielder TJ, Hoang YD, Lim J, McConnachie LA, Kavanagh TJ, et al. Lack of Maternal Glutamate Cysteine Ligase Modifier Subunit (*Gclm*) Decreases Oocyte Glutathione Concentrations and Disrupts Preimplantation Development in Mice. Endocrinology. 2011;152:2806-15.

[47] Cooper RL, Goldman JM, Vandenbergh JG. Monitoring of the Estrous Cycle in the Laboratory Rodent by Vaginal Lavage. In: Heindel JJ, Chapin RE, editors. Female Reproductive Toxicology. San Diego: Academic Press, Inc; 1993. p. 45-55.

[48] NRC. Guide for the Care and Use of Laboratory Animals. 8 ed. Washington, DC: National Research Council, National Academy of Sciences, National Academies Press; 2011.

[49] Pedersen T, Peters H. Proposal for a Classification of Oocytes in the Mouse Ovary. J Reprod Fertil. 1968;17:555-7.

[50] Plowchalk DR, Smith BJ, Mattison DR. Assessment of Toxicity to the Ovary Using Follicle Quantitation and Morphometrics. In: Heindel JJ, Chapin RE, editors. Female Reproductive Toxicology. San Diego, CA: Academic Press; 1993. p. 57-68.

[51] Safranski TJ, Lamberson WR, Keisler DH. Correlations among Three Measures of Puberty in Mice and Relationships with Estradiol Concentration and Ovulation. Biol Reprod. 1993;48:669-73.

[52] Lara H, E, McDonald JK, Ahmed CE, Ojeda SR. Guanethidine-Mediated Destruction of Ovarian Sympathetic Nerves Disrupts Ovarian Development and Function in Rats. Endocrinology. 1990;127:2199-209.

[53] Parsons BL, Manjanatha MG, Myers MB, McKim KL, Shelton SD, Wang Y, et al. Temporal Changes in K-*ras* Mutant Fraction in Lung Tissue of Big Blue B6C3F1 Mice Exposed to Ethylene Oxide. Toxicol Sci. 2013;136:26-38.

[54] McKinzie PB, Parsons BL. Accumulation of K-*Ras* Codon 12 Mutations in teh F344 Rat Distal Colon Following Azoxymethane Exposure. Environ Mol Mutagen. 2011;52:409-18.

[55] McKinzie PB, Delongchamp RR, Chen T, Parsons BL. ACB-PCR Measurement of K-*ras* Codon 12 Mutant Fractions in Livers of Big Blue Rats Treated with *N*-hydroxy-2-acetylaminofluorene. Mutagenesis. 2006;21:391-7.

[56] Ortiz L, Nakamura BN, Lim J, Li X, Blumberg B, Luderer U. In Utero Exposure to Benzo[a]pyrene Increases Adiposity and Causes Hepatic Steatosis in Female Mice and Glutathione Deficiency Is Protective. Toxicol Lett. 2013;223:260-7.

[57] Nathan BM, Hodges CA, Supelak PJ, Burrage LC, Nadeau JH, Palmert MR. A Quantitative Trait Locus on Chromosome 6 Regulates the Onset of Puberty in Mice. Endocrinology. 2006;147:5132-8.

[58] Ahima RS, Dushay J, Flier SN, Prabakaran D, Flier JS. Leptin Accelerates the Onset of Puberty in Normal Female Mice. J Clin Invest. 1997;99:391-5.

[59] Biegel LB, Flaws JA, Hirshfield AN, O'Connor JC, Elliott GS, Ladics GS, et al. 90-Day Feeding Study and One-Generation Reproduction Study in Crl:CD BR Rats with 17β-Estradiol. Toxicol Sci. 1998;44:116-42.

[60] Chapin RE, Harris MW, Davis BJ, Ward SM, Wilson RE, Mauney MA, et al. The Effects of Perinatal/Juvenile Methoxychlor Exposure on Adult Rat Nervous, Immune, and Reproductive Function. Fundam Appl Toxicol. 1997;40:138-57.

[61] Gray LE, Jr., Ostby J, Ferrell J, Rehnberg G, Linder R, Cooper R, et al. A Dose-Response Analysis of Methoxychlor-Induced Alterations of Reproductive Development and Function in the Rat. Fundamental and Applied Toxcicology. 1989;12:92-108.

[62] van Lipzig MMH, Vermeulen NPE, Gusinu R, Legler J, Frank H, Seidel A, et al. Formation of Estrogenic Metabolites of Benzo[a]pyrene and Chrysene by Cytochrome P450 Activity and Their Combined and Supra-maximal Estrogenic Activity. Environ Toxicol Pharmacol. 2005;19:41-55.

[63] Plíšková M, Vondráček J, Vojtěšek B, Kozubík A, Machala M. Deregulation of Cell Proliferation by Polycyclic Aromatic Hydrocarbons in Human Breast Carcinoma MCF-7 Cells Reflects Both Genotoxic and Nongenotoxic Events. Toxicol Sci. 2005;83:246-56.

[64] Weldy CS, White CC, Wilkerson H-W, Larson TV, Stewart JA, Gill SE, et al. Heterozygosity in the Glutathione Synthesis Gene Gclm Increases Sensitivity to Diesel Exhaust Particulate Induced Lung Inflammation in Mice. Inhal Toxicol. 2011;23:724-35.

654 **Table 1: *Kras* codon 12 mutant fractions by *Gclm* genotype and BaP dose**

Treatment	Genotype	*Kras* Codon 12 GAT Geometric Mean MF	*Kras* Codon 12 GAT Median MF	*Kras* Codon 12 GTT Geometric Mean MF	*Kras* Codon 12 GTT Median MF
Oil	***Gclm* +/+**	6.11×10^{-5}	6.12×10^{-5}	1.07×10^{-4}	1.09×10^{-4}
	***Gclm* +/-**	5.50×10^{-5}	5.59×10^{-5}	7.48×10^{-5}	6.62×10^{-5}
	***Gclm* -/-**	7.18×10^{-5}	4.69×10^{-5}	1.68×10^{-4}	1.97×10^{-4}
BaP	***Gclm* +/+**	4.04×10^{-5}	3.16×10^{-5}	7.42×10^{-5}	6.21×10^{-5}
	***Gclm* +/-**	4.42×10^{-5}	1.47×10^{-5}	8.55×10^{-5}	6.19×10^{-5}
	***Gclm* -/-**	3.16×10^{-5}	2.83×10^{-5}	8.45×10^{-5}	7.08×10^{-5}

655

656

Figure Legends

Figure 1: Prenatal BaP exposure leads to earlier onset of puberty. *Gclm+/+, Gclm+/-,* and *Gclm-/-* littermate female mice were exposed via oral dosing of their mothers with 0 or 2 mg/kg/day BaP daily from GD 6.5 through 15.5 and were followed from PND 21 for vaginal opening and first estrus as detailed in Materials and Methods. (A) Mean ± SEM age at vaginal opening ($P<0.001$, effects of *Gclm* genotype and BaP dose x genotype interaction). (B) Mean ± SEM age at first estrus ($P<0.001$, effect of BaP). (C) Mean ± SEM body weight at vaginal opening ($P\leq0.005$, effects of BaP dose, genotype, and dose x genotype interaction). (D) Mean ± SEM body weight at first estrus ($P<0.001$, effects of genotype and genotype x dose interaction; $P=0.014$, effect of BaP dose). N = 6-8 litters (7-16 offspring) per group.

Figure 2: Maternal *Gclm* heterozygosity does not modify the effects of prenatal BaP exposure on F1 ovarian follicle counts. F1 female mice were exposed prenatally to BaP as for Figure 1. The graphs show means ± SEM number of healthy follicles/ovary in *Gclm+/-* F1 daughters of *Gclm+/-* F0 mothers (left hand graphs) or C57BL/6J wild type F1 daughers of C57BL/6J F0 mothers at 6-7 weeks of age. (A,B) Primordial follicles. (C,D) Primary follicles. (E,F) Secondary follicles. (G,H) Antral follicles. N=4-5/group. *$P<0.05$ compared to 0 mg/kg group.

Figure 3. Distributions of ovarian *Kras* codon 12 GAT and GTT mutant fractions among experimental groups. ACB-PCR was used to measure the *Kras* codon 12 GAT and GTT MFs in the ovarian DNA of mice exposed prenatally to BaP or sesame oil vehicle as for Figure 1. (A) Images of 8% non-dematuring polyacrylamide gels used to resolve ACB-PCR products for quantification of MF. (B) Mean ± SEM of MFs from duplicate DNA samples per ovary for each animal by genotype and treatment group.

Figure 4. No effects of prenatal BaP exposure or *Gclm* genotype on ovarian *Kras* codon 12 GAT and GTT mutant fraction. Means ± SEM MF distributions for *Kras* codon 12 GAT mutation (A) and GTT mutation (B) by treatment group in the same samples as in Figure 3. There were no statistically significant effects of BaP treatment or genotype by 2-way ANOVA.

Figure 5. Ovarian *Kras* GAT and GTT mutations are highly correlated within ovaries. The correlation between the *Kras* codon 12 GAT and GTT Log_{10} MF measurements within individual mouse ovary DNA samples (Pearson $r = 0.8504$, $P < 0.0001$, two-tailed test).

Figure 1

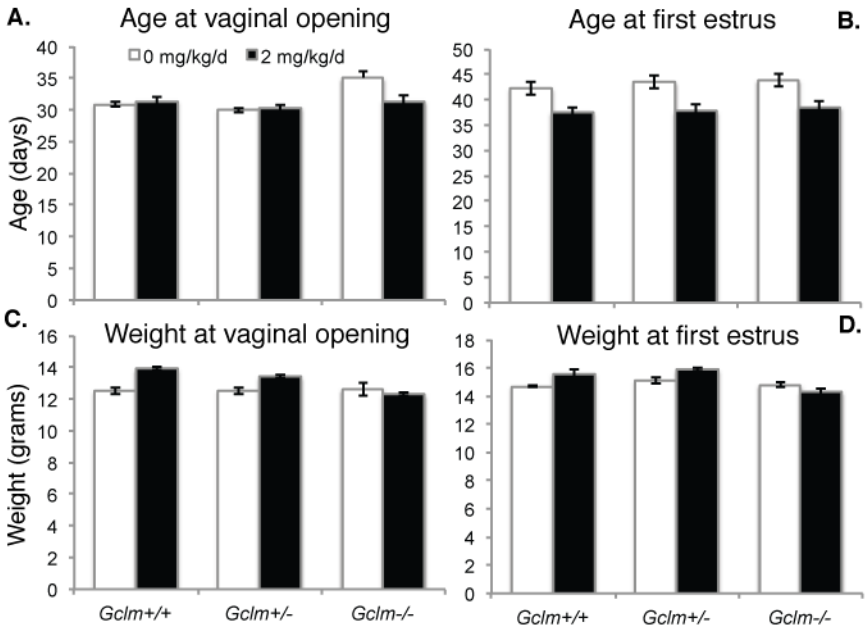
A.
Age at vaginal opening
0 mg/kg/d
2 mg/kg/d
Age (days)
B.
Age at first estrus
C.
Weight at vaginal opening
Weight (grams)
D.
Weight at first estrus
Gclm+/+
Gclm+/-
Gclm-/-

Figure 2

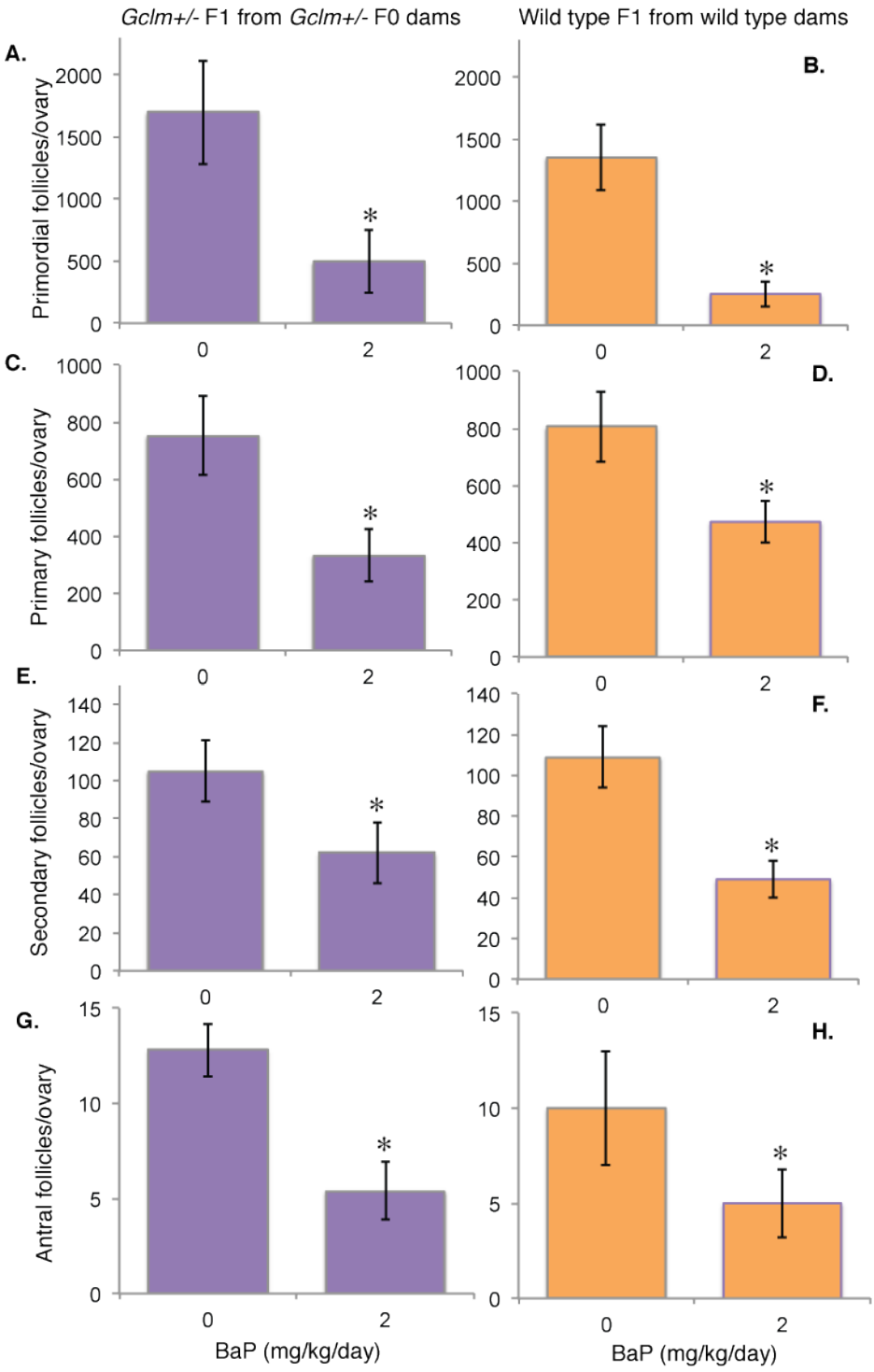
Gclm+/- F1 from *Gclm+/-* F0 dams
Wild type F1 from wild type dams
A.
B.
C.
D.
E.
F.
G.
H.
Primordial follicles/ovary
Primary follicles/ovary
Secondary follicles/ovary
Antral follicles/ovary
BaP (mg/kg/day)
BaP (mg/kg/day)

Figure 3

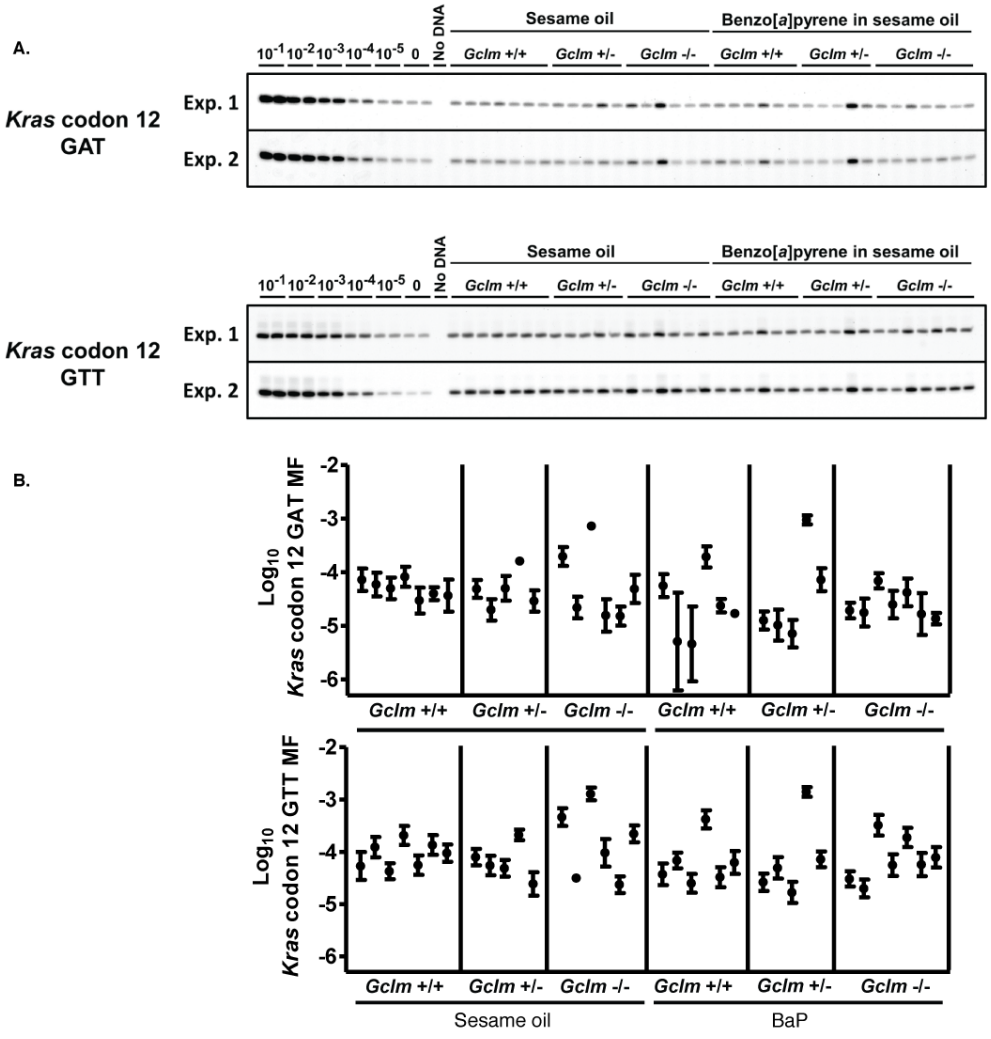
A.
Sesame oil
Benzo[a]pyrene in sesame oil
No DNA
10-1 10-2 10-3 10-4 10-5 0
Gclm +/+
Gclm +/-
Gclm -/-
Kras codon 12 GAT
Exp. 1
Exp. 2
Kras codon 12 GTT
B.
Log10 Kras codon 12 GAT MF
Log10 Kras codon 12 GTT MF
-2
-3
-4
-5
-6
Sesame oil
BaP

700 **Figure 4**

701

702

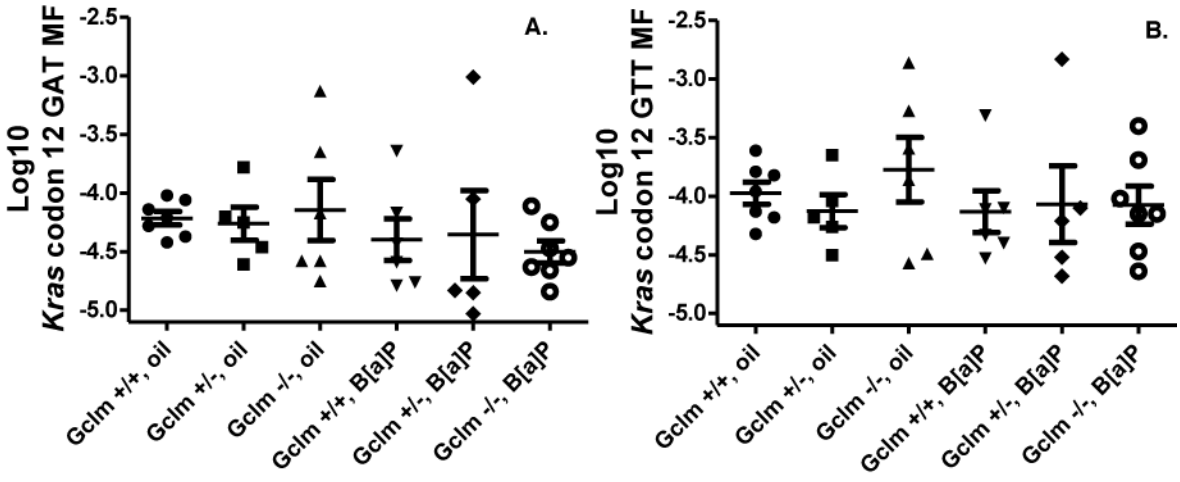

703

Figure 5

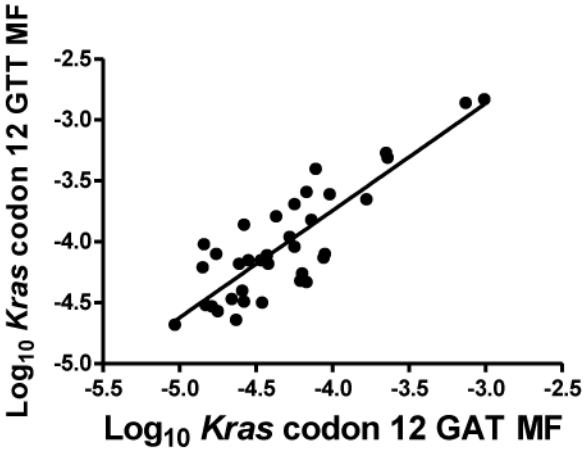
Log10 Kras codon 12 GTT MF
-2.5
-3.0
-3.5
-4.0
-4.5
-5.0
-5.5
-5.0
-4.5
-4.0
-3.5
-3.0
-2.5
Log10 Kras codon 12 GAT MF